Stability of ZnO{0 0 0 1} against low energy ion bombardment

A. Sulyok[a], M. Menyhard[a] and J.B. Malherbe[b]

[a]Research Institute for Technical Physics and Materials Science, P.O. Box 49, H-1525 Budapest, Hungary

[b]Department of Physics, **University of Pretoria**, Pretoria 0002, South Africa

Abstract

The steady-state surface compositions of the polar (O and Zn terminated) faces of ZnO{0 0 0 1} produced by low energy (0.3–2 keV) Ar^+ ion bombardment were studied by Auger electron spectroscopy and electron energy loss spectroscopy. The alterations produced by the ion bombardment using different ion energies were monitored by calculating the intensity ratios of the low and high energy Zn Auger peaks (59 eV and 994 eV, respectively); Zn and O Auger peaks (59 eV and 510 eV, respectively). Based on the dependence of these ratios on the ion energy and termination of the surface, we could conclude that the stability of the Zn face is higher against the low energy argon ion bombardment-induced compositional changes than that of the O face.

Article Outline

1. Introduction

The material properties of ZnO make it a candidate for a very large variety of applications [1], [2] and [3]. In optoelectronic applications, ZnO has many advantages compared to competing compound semiconductor materials currently in use. It is a direct, wide band-gap semiconductor with E_g = 3.37 eV. This wide band-gap gives it the potential for electroluminescence in the blue and UV region. ZnO is a II–VI compound semiconductor whose ionicity is at the borderline between a covalent and an ionic semiconductor. At room temperature, the thermodynamical stable phase is hexagonal wurtzite structure where each anion is surrounded by four cations of a tetrahedron, and vice versa [1]. This means that ZnO{0 0 0 1} exhibits either a Zn or an O terminated surface. Furthermore, ZnO is one of the hardest of the II–VI family of semiconductors. This means that it will not be degraded as easily as the other compounds through the appearance of defects. Recently, it has been shown that ZnO is very resistant to high energy irradiation (making it a possible candidate for electronic devices in space applications) [1] that assumes an efficient way of damage recovery. This recovery can, even at room temperature, prevent the amorphisation of crystal at large fluences [2]. Unlimited damage accumulation can be achieved only if chemical interaction takes place between the lattice and the implanted ions [4]. On the other hand, it has been shown [5] that with quenching the dynamic annealing of the lattice, the damage recovery is limited though starts over 80–130 K. The once generated defect complexes can be annealed only at very high temperatures.

There are only a few studies dealing with the effect of low energy ion bombardment to ZnO. Using X-ray photoelectron spectroscopy (XPS) Kim et al. [7] found that Ar^+ bombardment did not influence the surface stoichiometry. Not much information is given about the bombardment conditions, but it seems as if the ion energy was between 0.2 and 1 keV.

There have been a number of studies where ZnO was subjected to reactive plasma etching. It was found by AES analyses that the ZnO surfaces remained stoichiometric after $CH_4/H_2/Ar$ [8] and $BCl_3/Cl_2/Ar$ etching [9]. However, reactive plasma etching with Cl_2/Ar at elevated temperatures (150 °C and 300 °C) showed the surface to become Zn-enriched and roughened as well [10]. A photoluminescence (PL) study on $CH_4/H_2/Ar$

etched ZnO showed that the PL signals change and scaled with ion energy up to 250 eV, and saturated for larger energies. This is ascribed to more efficient dynamic annealing of bombardment-induced point defects at a higher defect production rate, producing essentially a saturation damage level [8]. Based on these studies, we do not know if dynamic self-recovery works in the surface close region, where the processes might be affected by the interaction with the surface.

There is a long history (e.g., [6]) of studies concerning the explanation of the bombardment-induced surface compositional changes in oxides ([11], [12], [13], [14] and [15]). In all these studies it was found that if there are any surface compositional changes, then oxygen was preferentially lost from the oxide surface.

Additional interesting question is if the surface alteration due to ion bombardments depends on the polarity of the surface. In recent work, it has been shown that in the case of SiC, the ion bombardment-induced damage strongly depends on the polarity of the surface [16].

In this paper, we report on the steady-state composition of the two (0 0 0 1) (Zn terminated) and (0 0 0-1) (O terminated) faces produced by low energy (0.3–2 keV) grazing angle bombardment by Ar^+. It is shown that the surface alteration is not as pronounced as in SiC, and that the Zn terminated face is more resistant to alteration by the ion bombardment, than the O face.

2. Experimental

Two slices with orientation of (0 0 0 1) (Zn terminated) and (0 0 0-1) (O terminated) were cut from a ZnO single crystal. Both slices were polished and cleaned in the usual manner. They were mounted side by side to the sample holder with oxygen and zinc terminated faces up, respectively. This way, the ion bombardment and data collection by electron spectroscopy took place in identical circumstances of the two surfaces. The electron spectroscopy measurement included Auger electron spectroscopy (AES) analysis and electron energy loss spectroscopy (EELS).

Our aim was to determine the steady-state condition of the two faces of the ZnO crystal for various ion bombardment conditions. According to our usual AES depth profiling protocol, sequential ion bombardment and AES measurement were carried out and the

AES “depth profile” was recorded. The part of the depth profile, which was kept for further analysis, was the one where the peak height ratios of the measured elements did not change with time. We took 10–15 points in this part of the “depth profile” and the peak height ratios were averaged to get the steady-state composition. The standard deviation of the averaged points was always less than 3%.

The AES analysis was carried out by means of a DESA 100 (STAIB) electron spectrometer. The mean angle of detection slit is 25° relative to the surface normal. This geometry results in that the information depth for a given Auger-signal is 0.91 times the inelastic mean free paths (IMFP) of Auger electrons, neglecting the elastic scattering correction. The resolution of this spectrometer can be electronically adjusted and was chosen to be 1 eV and 4 eV under and above 100 eV, respectively. The direct spectrum was measured and later it was numerically differentiated. The intensity of the Auger peak is given as the peak-to-peak amplitude measured in the differentiated spectrum. The following Auger peaks have been measured: Zn MMM transition 59 eV, O KLL transition at 516 eV and Zn LMM transition at 994 eV. The Zn peak energies were calibrated against the values given in Davis et al. [17]. The low and high energy Zn Auger peaks were measured to probe various depths of the material in the same time. Energy loss spectra have been measured applying the same conditions as was applied to measure the Auger spectra. Accordingly, the direct spectrum was detected on the ZnO faces after stationary composition was reached. The elastic peak together with the nearby loss spectra were recorded. The energy of the primary electron beam was 300 eV to assure a small information depth.

Ion bombardment for both types of measurements was applied by using the following conditions: projectile Ar^+, energy 300–2000 eV, angle of incidence 78–86° (with respect to the surface normal). The ion current density was estimated to be 5×10^{-6} A/cm^2. During a pre-treatment of surface, the specimen was rotated during ion bombardment to avoid the unwanted morphology development before any measurement. During the actual AES “depth profiling”, the specimen was not rotated to reduce the noise.

3. Results and discussion

Fig. 1 shows the steady-state peak height ratios measured on the two (zinc and oxygen terminated) surfaces of the ZnO crystal as a function of the ion energy. The ratios of high energy Zn Auger peak to the oxygen Auger peak (curves with square and circle symbols in Fig. 1) show constant values within the accuracy of measurement versus ion energy. The IMFP for the high energy zinc and oxygen Auger electrons are 19.5 Å and 12.4 Å [18], respectively. This means these Auger electrons originate from a relatively thick region 5–7 atomic layer pairs in average. We can conclude based on the ion energy independent Zn(996)/O peak height ratios that the average composition of this thick region does not depend either on the ion energy or on the termination of the surface.

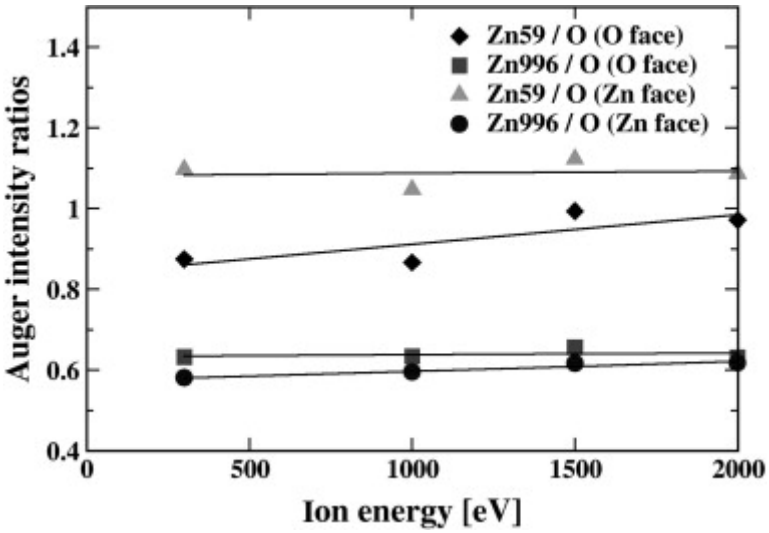

Fig. 1. Auger peak height ratios measured on stationary surface of ion bombarded ZnO versus ion energy. The Auger peaks were detected on opposite (0 0 0 1) faces (O face and Zn face) of the ZnO crystal. The measured values indicated by symbols while the lines are only to lead the eyes.

On the contrary, if we consider the Auger peak height ratio of low energy zinc to the oxygen one, a dependence on the ion energy is found and the ratios measured on different terminations seem significantly different. Because the IMFP of the low energy zinc Auger electron is only 4.4 Å [18], the ratios using the low energy Zn peak are more sensitive to the surface compositional changes. Thus, we can conclude that the stationary composition of the topmost atomic layers depend on the ion energy and the termination

of the crystal as well. Accordingly, the ratio of the peak heights of low-energy zinc to the high-energy one depends on the ion energy and termination of the surface as well (Fig. 2). The Zn(59)/Zn(994) ratio is almost constant on the Zn side and increasing with ion energy on the O side.

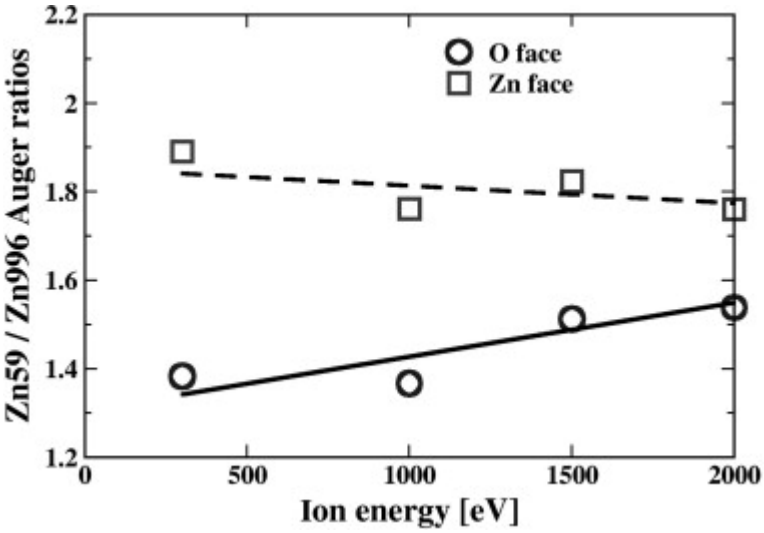

Fig. 2. Zn(59 eV)/Zn(996 eV) Auger peak height ratios versus ion energy measured on O face and Zn face of ZnO. The lines are only to lead the eyes.

To characterize the difference of the steady-state conditions of the Zn and O terminated surfaces, the excess quantities are introduced as ratios of the above ratios measured on the two differently terminated surface, that is, e.g.,

$Zn(59)/Zn(996)_{ex} = Zn(59)/Zn(994)_{Znface}/Zn(59)/Zn(994)_{Oface}$.

Fig. 3 shows the excess quantities as a function of the ion energy. These quantities show a clear dependence on the ion energy. The relative enrichment of Zn on the Zn terminated surface with respect to that on the O terminated surface increases with decreasing ion energy. This kind of behaviour is similar to that observed on SiC [16].

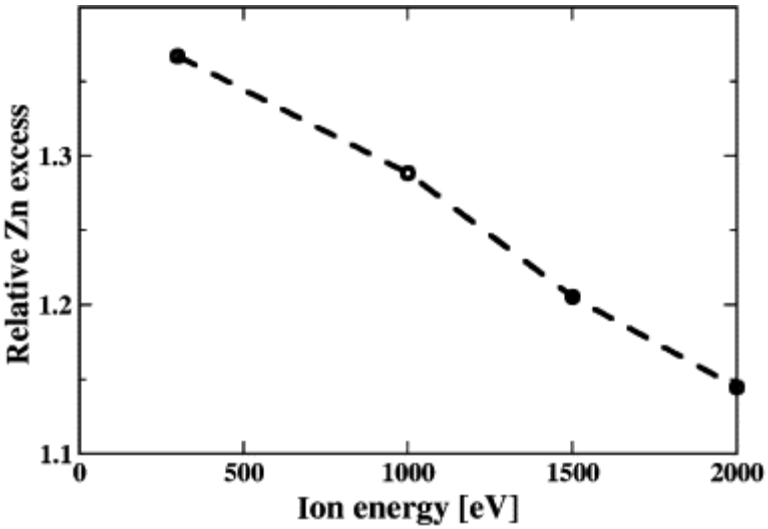

Fig. 3. Relative Zn enrichment at bombarded surface; calculated from the Zn(59 eV)/Zn(996 eV) ratios measured on the Zn face and the O face, respectively.

Though the measured Auger intensities cannot be directly inverted to reveal the actual concentration distribution in the near surface region it is possible to find by means of trial-and-error method such a composition distribution which results the same intensities as the measured one. If this distribution is a reasonable one, we can accept it as the model of the real one.

The Zn/O ratios were calculated for the actual geometrical arrangement assuming that:

• the electron attenuation is described by IMFP,

• the ZnO material can be described by a series of bilayers, according to its crystal structure at the {0 0 0 1} face. We used the following real crystal parameters: the thickness of bilayers is 2.7 Å and the oxide plane is shifted by 0.83 Å to the Zn plane up or down at the Zn and O faces, respectively,

• the emitted Auger electrons are attenuated by the bilayers; the attenuation is calculated in discrete steps for each bilayer,

• Auger electrons starting from a bilayer may suffer some attenuation η already inside the bilayer if the electron was emitted by the lower atomic layer of the bilayer. The emission of the upper layer takes place without weakening. Accordingly η is less than one or equals to one, respectively. The attenuations κ in the following layers are identical, disregarding the origin of place.

Thus, the total detected Auger current I was calculated as the sum of emitted Auger sources.

$$I_{\mathrm{loZn,Oface}} = \sum_{j} I_j \eta_{\mathrm{loZn,Oface}} \kappa_{\mathrm{loZn}}^{j-1}$$

For example, the expression is for low energy Zn peak at the O face is as: where I_j is the emission intensity at layer j; $\eta_{\mathrm{loZn,Oface}}$ is the attenuation of electron intensity in the bilayers of origin, regarding the low energy Auger peak of Zn and the Zn position in the bilayer at O face; κ_{loZn} is the attenuation of low energy Zn Auger peak when passing through a bilayer. The intensity of Auger emission at layer j was constant at layers in the bulk, but it was different at the surface layer (j = 1) according to their composition. Otherwise, it means we neglected the attenuation of primary beam with depth. This is a reasonable simplification because the Auger energies we observed are much lower then the primary energy 5 keV.

The attenuation κ was found as 0.54, 0.87 and 0.80 for low Zn, high Zn and O peaks, respectively. The starting attenuation η was found to be 0.88, 0.97 and 0.94 for low Zn, high Zn and O peaks, respectively, when they were in lower position in the bilayer. At the opposite faces, when they were in upper position in the bilayer, η is necessarily 1 for all cases. Hence, the expression gives different intensities for the different faces because of the conditions applied.

If we assume that the damage at 300 eV ion bombardment is negligible, we can fit the η value to get the measured intensities. Interestingly, if we used that amount of attenuation from the lower atomic plane of the bilayer that would be valid for a 0.83 Å thick homogeneous ZnO layer practically the same value is reached. This would support the validity of this simplified calculation. Having η value we can apply our equation to find in-depth concentration distributions providing the same intensities as the measured ones. Additional information is that the high energy Zn/O ratio hardly changes with the ion energy; thus, we can assume that the composition change took place at the very surface. Thus, all changes are confined to the very first atomic layer. Thus, we could calculate compositions for both surfaces for all ion energies. As it is clear from the above, there is no change in the very first atomic layer (and obviously in the deeper ones) of the Zn face

up to 2 keV Ar^+ bombardment, while at the O face, the composition was found to be $Zn_{0.58}O_{0.42}$ for 1 and 2 keV energy bombardments. In other words, in the first double layer the number of Zn atoms equal while the number of O atoms are 27% less than in a bulk double layer, accordingly.

The electron transport and thus, the measurable losses in the reflected electron spectrum (REELS) depend on the material and electronic structure of the near surface region. We have measured the reflected electron spectra of 300 eV primary electrons, impinging upon the surface at an angle of 65° (with respect to the surface normal) on both faces, after steady-state conditions appeared for each of the four different ion energies used in this study. The loss spectra were not sensitive to the variation of ion energy on either of the faces. On the other hand, the two faces provided slightly different loss spectra. The loss spectra between 0 and 25 eV normalized for identical elastic peak area are shown in Fig. 4. The features on the spectra can be identified as follows. The dominant loss at 18 eV is a bulk plasmon loss [19] and [20]. The peak at 9.5 eV is identified as a surface plasmon loss [20]. Because ion beam damage observed by Auger peaks does not effect the loss peaks (within our sensitivity) we have to conclude that the change in electronic structure caused by ion beam is minor. It is clear that the surface plasmon difference at the two faces needs further studies.

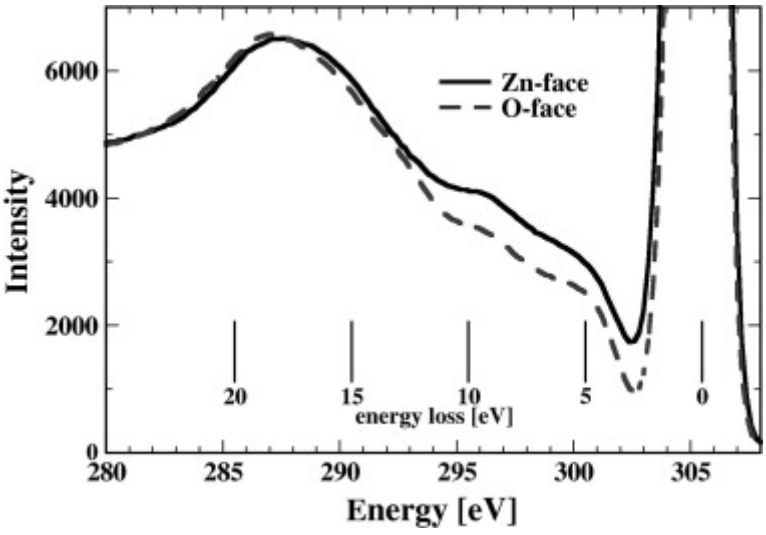

Fig. 4. Loss part of electron spectra measured on O face and Zn face of ZnO at about 300 eV primary energy. The normal energy axes show the detected energy. The internal energy axes is scaled according to the energy loss.

4. Conclusions

The AES and energy loss spectroscopy measurements showed that the ZnO(0 0 0 1) surface is relatively resistant to the low energy argon ion bombardment – induced compositional changes. While composition of Zn face is not influenced by the ion bombardment within the sensitivity of AES analysis, the O face showed some O deficiency for 1 and 2 keV bombardment. The bulk plasmon loss did not depend on the ion bombardment induced damage, while the surface plasmon was found to be different on the Zn and O terminated surfaces.

References

[1] Ü. Özgür, Ya. I. Alivov, C. Liu, A. Teke, M.A. Reshchikov, S. Doğan, V. Avrutin, S.-J. Cho and H. Morkoc, *J. Appl. Phys.* **98** (2005), p. 041301-1.

[2] E. Rita, E. Alves, U. Wahl, J.G. Correia, T. Monteiro, M.J. Soares, A. Neves and M. Peres, *Nucl. Instrum. Meth. B* **242** (2006), p. 580.

[3] S.J. Pearton, D.P. Norton, K. Ip, Y.W. Heo and T. Steiner, *J. Vac. Sci. Technol. B* **22** (2004), p. 932.

[4] S.O. Kucheyev, J.S. Williams and C. Jagadish, *Vacuum* **73** (2004), p. 93.

[5] K. Lorenz, E. Alves, E. Wendler, O. Bilani, W. Wesch and M. Hayes, *Appl. Phys. Lett.* **87** (2005), p. 191904.

[6] J.B. Malherbe, *Critical Rev. Solid State Mater. Sci.* **19** (1994), p. 129.

[7] K.S. Kim, W.E. Baitinger, J.W. Amy and N. Winograd, *J. Electronspectrosc. Related Phenom.* **5** (1974), p. 351.

[8] K. Ip, K.H. Baik, M.E. Overberg, E.S. Lambers, Y.W. Heo, D.P. Norton, S.J. Pearton, F. Ren and J.M. Zavada, *Appl. Phys. Lett.* **81** (2002), p. 3546.

[9] H.-K. Kim, J.W. Bae, T.-K. Kim, K.-K. Kim, T.-Y. Seong and I. Asesida, *J. Vac. Sci. Technol. B* **21** (2003), p. 1273.

[10] W.T. Lim, K.H. Baek, J.W. Lee, E.S. Lee, M.H. Jeon, G.S. Cho, Y.W. Heo, D.P. Norton and S.J. Pearton, *Appl. Phys. Lett.* **83** (2003), p. 3105.
[11] I. Bertóti, R. Kelly, M. Mohai and A. Tóth, *Surf. Interface Anal.* **19** (1992), p. 291.
[12] I. Bertóti, R. Kelly, M. Mohai and A. Tóth, *Nucl. Instrum. Meth. Phys. Res.* **B80/81** (1993), p. 1219.
[13] J.B. Malherbe, S. Hofmann and J.M. Sanz, *Appl. Surf. Sci.* **27** (1986), p. 355.
[14] D.F. Mitchell, G.I. Sproule and M.J. Graham, *Surf. Interface Anal.* **15** (1992), p. 487.
[15] R. Kelly and A. Miotello, *Nucl. Instrum. Meth. Phys. Res.* **B122** (1997), p. 374.
[16] L. Kotis, A. Sulyok, M. Menyhard, J.B. Malherbe and R.Q. Odendaal, *Appl. Sur. Sci* **252/5** (2005), p. 1785.
[17] L.E. Davis, N.C. MacDonald, P.W. Palmberg, G.E. Riach, R.E. Weber, Handbook of Auger Electron Spectroscopy, Physical Electronics, 2nd print, 1978.
[18] NIST Database on IMFP.
[19] R.L. Hengehold, R.J. Almassy and F.L. Pedrotti, *Phys. Rev. B* **1** (1970), p. 4784.
[20] Y. Ding and Z.L. Wang, *J. Elect. Microsc.* **54** (2005), p. 287.

Corresponding author.